DOI: 10.13009/EUCASS2023-493
Aerospace Europe Conference 2023 – 10TH EUCASS – 9TH CEAS

Feasibility study for a medium-range regional aircraft retrofit with battery powered propulsion system

Jonas Ludowicy⋆†, *Victor Bahrs*⋆, *Martin Staggat*⋆
⋆*German Aerospace Center (DLR) - Institute of Electrified Aero Engines, Lieberoser Str. 13a, 03046 Cottbus, Germany*
jonas.ludowicy@dlr.de
†Corresponding author

Abstract

In this paper battery-electric retrofits for a medium-range regional aircraft, comparable to the ATR 42-500, are analysed for five different technology scenarios. The methodology and component models are described in detail as well as the validation of both the methodology and the aircraft model against conventionally powered aircraft. Based on the assumptions used, the present study reveals that battery-electric retrofits are likely not possible in the near-term future. Only when heavily relaxing the mission requirements and significantly decreasing the range retrofits become possible. For a 2050 technology scenario the range of the battery-electric retrofit is only about 280 km.

1. Introduction

In recent years, the aviation industry has been striving to reduce its carbon footprint and environmental impact while improving its operational efficiency and reducing cost. Conventional technology and evolutionary improvement will not be sufficient to fulfill the goals set in the Flightpath 2050 [1] report. For maximum impact revolutionary new technology is needed as projected by the ATAG [2].

One of the promising solutions that have emerged in response to these challenges is the development of electric and hybrid-electric aircraft propulsion systems. Aircraft equipped with such propulsion systems have the potential to reduce greenhouse gas emissions, noise pollution, and operating costs compared to conventional fossil fuel-powered aircraft [3, 4]. Battery powered electric aircraft even eliminate all local emissions except waste heat and noise.

In general aviation, first battery aircraft are commercially available, e.g. the Pipistrel Velis Electro. This aircraft offers a range of 50 min and a payload capacity of up to two passengers [5]. Battery electric commuter class aircraft with up to 9 passengers are in development [6]. The environmental impact of such aircraft on the global scale is likely not very large, their share in global CO_2 emissions is not even included in the study by Graver *et al.* [7]. Regional aircraft, being the next larger category and logical next step to introduce battery based electric propulsion, are estimated with a share of still only 5 % of aviation CO_2 emissions [7]. However, there are use cases for short routes that might be ideal to be operated by an electric regional aircraft [8]. In general, flights with a distance less than 1500 km account for about 25 % of the total passenger carbon dioxide emissions in aviation [7]. Therefore, economically beneficial electrified regional aircraft that are able to serve these routes offer a significant overall aviation emissions reduction potential.

Electric powertrains bring new challenges. On the one hand, electric powertrains are benefiting from significantly higher conversion efficiencies in comparison to conventional engines. On the other hand, the inhibiting factor for a wider use of battery-electric propulsion in all aircraft classes is the battery technology [9]. Therefore, the improvement of available batteries is a key factor in the feasibility of electric aircraft propulsion. A continuous development has already led to the production of more efficient and lightweight batteries with higher energy densities [10]. Through further improvement in battery technology, electric aircraft with higher range and payload can be expected to be viable.

Several studies have been conducted on the feasibility of battery-powered regional aircraft. Anker and Noland [11] analysed the propulsion system for a 50 passenger aircraft with a 400 km range including reserves. Since the battery increased the aircraft mass to double the mass of the conventional counterpart, purely battery-electric propulsion does not seem possible based on current technology. Only the most optimistic assumptions for 2030 technologies (500 Wh/kg batteries, 20 kW/kg power electronics and 13 kW/kg motors) yielded a viable design for the powertrain. The study assumed constant efficiencies for the powertrain components and only analysed the cruise phase, neglecting high power phases such as take-off and climb that are crucial for battery sizing.

DOI: 10.13009/EUCASS2023-493

Baerheim *et al.* [12] also analysed a regional aircraft retrofit for multiple missions with 39 passengers and up to about 400 km range. They included all mission phases and as well as a reserve. Take-off and climb were always the most power demanding part of the flight. In their study they assumed constant propulsion system component efficiencies and the same mass for the electric propulsion system as for the conventional engines. Again, only for the most optimistic technology assumption (1000 Wh/kg batteries) the aircraft was feasible for the mission with about 400 km range.
In this paper, a study for battery-electric powertrain retrofits based on the medium-range regional aircraft ATR 42-500 is presented that is based on more sophisticated component models and includes a higher fidelity battery model. The paper will provide a description of the aircraft retrofit procedure, focusing on the propulsion system and battery technology used. A study investigating the possible range of battery-electric retrofits for different technology levels and development scenarios is presented. As preliminary results showed that the battery-electric retrofits for the original mission would be too heavy, the mission requirements were adapted. This also allows for a fair comparison of the aircraft with conventional and battery-electric powertrains, which is only possible with optimized missions for new powertrains [13].
In the next section the methodology used to simulate the aircraft and powertrain is described. The mission simulation is explained and validated with aircraft data similar to the ATR 42-500. In particular, the models used for the powertrain components are specified and described as well. Finally, the results of the technology study are presented and discussed.

2. Methodology

Hybrid- or fully-electric aircraft cannot be sized utilizing the same handbook methods and formulae used for conventionally powered aircraft described by Raymer, Gudmundsson or Torenbeek [14–16]. These propulsion systems cannot be modelled by a simple specific fuel consumption value and the aircraft weight might not change significantly over the mission, dependent on the hybridization and architecture of the powertrain. Instead, especially for sizing of the energy storage, new methods have to be used, e.g. described by Finger [17]. The method applied in this paper has been described and utilized for hybrid regional aircraft studies in Staggat *et al.* [18] and an overview of the sizing routine used in this study is depicted in Figure 1.
With the top level aircraft requirements (TLARs), mission description, aerodynamic information and initial assumptions for the masses from the aircraft model the powertrain can be sized. Its individual components and their models are described in the following subsection. During the mission simulation the necessary battery power is then calculated using the powertrain models. With the power profile over the mission the batteries can be sized with the three criteria explained further in section 2.1.3. The updated masses of powertrain and batteries are fed back to the aircraft model and the process is solved iteratively.

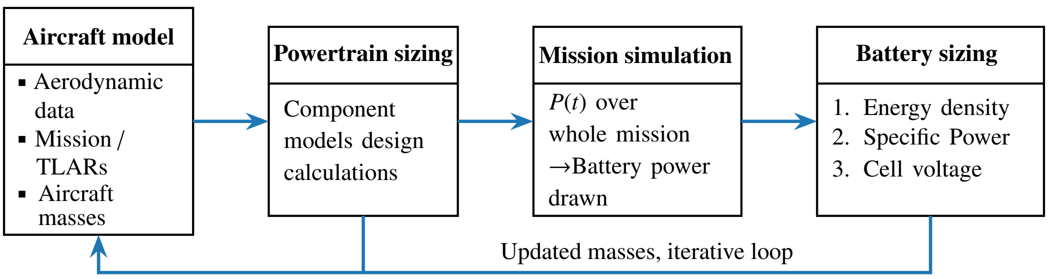

Figure 1: Sizing process overview

In the mission simulation the flight is subdivided in discrete time steps, where the required power in each step is calculated via an energy balance based on the equations of motion. The mission is divided into the take-off, climb, cruise and descent segment as shown in Figure 2. A reserve mission with another climb and diversion is not included in the flight profile but note that the cruise segment can be used to include extra reserves as additional range.
For the take-off phase, exemplary, the energy is calculated by

$$E_{TO} = E_{acc} + E_{grf} + E_{aerod}, \tag{1}$$

where E_{acc} is the energy required to accelerate the aircraft to the take-off reference speed, E_{grf} to overcome ground friction and E_{aerod} to account for aerodynamic drag. The calculation is based on formulae from Gudmundsson [15].
For all other phases only the aerodynamic drag and changes in potential energy are accounted for. Any energy required for acceleration is not considered in these phases. Aerodynamic drag calculations are based on a zero-lift drag coeffi-

DOI: 10.13009/EUCASS2023-493

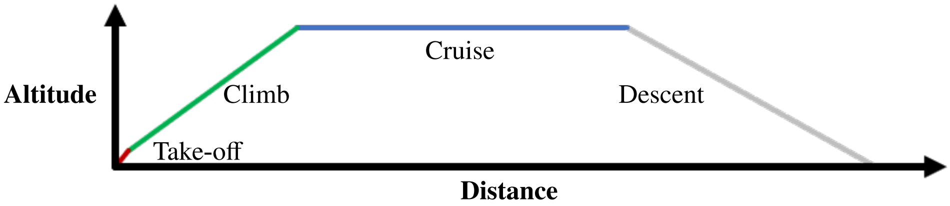

Figure 2: Illustration of assumed aircraft mission

cient plus induced drag. The required power in each time step is used to determine the corresponding energy carrier, battery or fuel mass.
The conventionally powered baseline aircraft, based on the ATR 42-500, is retrofitted with a battery-electric powertrain. The turboprop engines are replaced by the electric powertrains while the two propellers remain identical. The aircraft outer mold line, as well as the power-to-weight ratio, are also kept similar to the ATR 42-500. With the wing loading being fixed at the original value too, any impact of the new powertrain on the aircraft aerodynamics is not considered in the present study. A new empty mass of the aircraft is calculated deducting the mass of the two turboprop engines. This new empty mass will be used as a basis in the sizing processes for conventionally powered aircraft for validation purposes and the battery-electric powered aircraft.

2.1 Electric powertrain modelling

The chosen topology for this investigation of the electric powertrain is illustrated in Figure 3. The propeller is only modelled by a constant efficiency of $\eta = 0.8$ assuming a constant rotational speed during each flight phase. The propeller is connected to a gearbox with a fixed gear ratio of about 3.3, increasing the motor rotational speed to enable lighter motor designs. Within the gearbox model the mass estimation is based on Brown [19], the volume estimation on Reynolds [20] and the efficiency estimation on Neudorfer [21]. The assumed propeller rotational speeds are 2100 rpm for take-off, 1980 rpm during climb and 1800 rpm during cruise, translating to electric motor rotational speeds of 7000 rpm, 6600 rpm and 6000 rpm respectively. The motor is supplied with alternating current (AC) by an inverter. To enable a constant input voltage at the direct current (DC) power side of the inverter, a DC-DC-converter is used to supply the necessary bus voltage to the inverter. The voltage level of the DC bus is kept constant at 1.5 kV.
The losses of the components result in waste heat which has to be removed. These heat flows, originating from the gearbox, motor, inverter and converter, are removed by an active thermal management system (TMS). The parasitic power to operate the TMS must also be provided by the batteries. Note that the battery itself is assumed to be passively cooled and that the battery thermal management system mass is included in the battery pack level energy density. In the following subsections the component models are described in more detail.

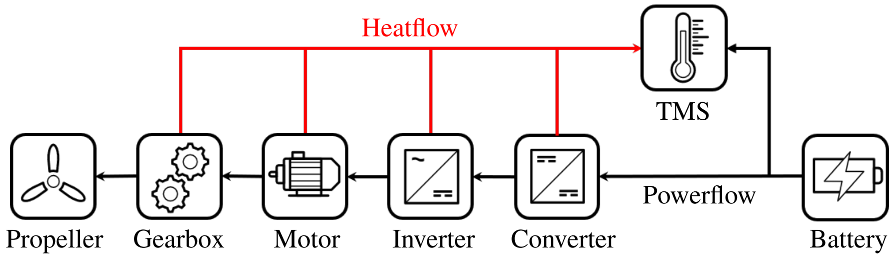

Figure 3: Electric powertrain topology

2.1.1 Motor modelling

The electric machines are modeled based on an analytical approach published by Bahrs *et al.* [22]. Here, a permanent magnet synchronous machine is used. The model provides the mass, volume and efficiency of the machine based on inputs regarding motor architecture, material properties and operating conditions.
In this study three-phase six-pole motors are assumed and designed for the installed power required to achieve the assumed aircraft power-to-weight ratio. A power factor of 90 % and a copper fill factor of 50 % are used. Magnets with a remanent field density of 1.25 T [23] and a height of 13 mm are assumed. The magnets are mounted to the rotor by a sleeve made of composite materials. Shaft, rotor and stator are assumed to be iron. The aforementioned inputs are considered to represent current state of the art technology.

DOI: 10.13009/EUCASS2023-493

In the sizing process the total motor mass is calculated by summing up all individual part masses. For the efficiency calculation electrical, magnetic, friction and electromagnetic losses are taken into account [22]. With the electric motor preliminary design and sizing, efficiency and performance maps are available as shown in Figure 4. These maps are used for all off-design calculations during the mission simulation.

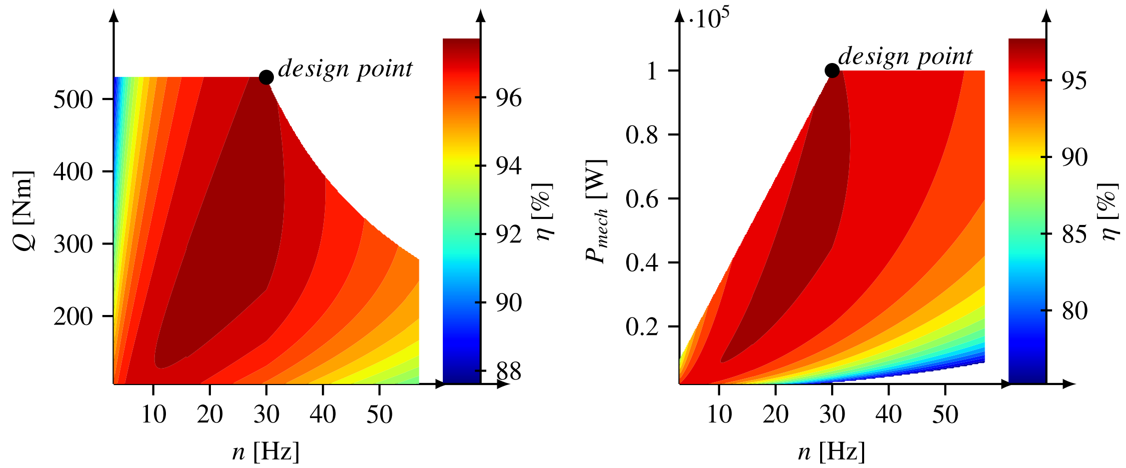

Figure 4: Efficiency, torque and power maps taken from Bahrs *et al.* [22]

2.1.2 Inverter and converter modelling

The inverters, connected to the electric machines, are modelled by a three level neutral point clamped (3L-NPC) topology. Semiconductor properties from data sheets are used to determine serial and parallel interconnection of the diodes and switches, based on the electric power demand of the motor. The inverter efficiency is calculated with the individual conducting and switching losses of all semiconductor elements [24]. Two DC link capacitors are considered at the inverter input, while between inverter and motor a filter is included to reduce harmonics. The filter for each phase consists of an inductor and a capacitor [25]. Mass and volume of the inverter are estimated based on the amount of semiconductors and the required capacitors and inductors at input and output [26].
To change the voltage level of the batteries, models for boost and buck converters are used. The converters raise or lower the voltage level provided by the battery to a constant voltage input level for the inverter. For this paper, the converters are modelled by a fixed power density and a constant efficiency of 98 %.

2.1.3 Battery modelling

Modelling the battery is done via a parameterized curve for the single cell voltage. The chosen regression curve of a lithium-ion battery cell was published by Chen and Rincon-Mora [27] and is depicted over the state of charge (SOC) in Figure 5. A reduction in nominal cell voltage can be observed for decreasing SOC of the battery.
The cell voltage is furthermore dependent on the current load. In general, the voltage rises when charging the battery and decreases when discharging the battery, as shown in Figure 5. The higher the current load I, the more the cell voltage increases or decreases. This relation is represented by

$$V_{discharge} = V_{oc} - R_{oc} \cdot I \tag{2}$$

and

$$V_{charge} = V_{oc} + R_{oc} \cdot I, \tag{3}$$

whereby V_{oc} and R_{oc} are the SOC dependent open cell voltage and resistance respectively [28]. Due to this load dependent behaviour of the batteries, the battery has to be sized after the mission simulation. With the load profile of the battery over the course of the mission the sizing routine iteratively adds cells in series or parallel to the battery to fulfill all power demands of the powertrain at every single time step during the mission. The battery sizing routine used is adapted from Vratny *et al.* [29].
The battery sizing is limited by three criteria, overall capacity, peak power and cell voltage. Regarding capacity, the SOC should never fall below 20 % to prevent a deep discharge of the battery that could permanently damage the cells

DOI: 10.13009/EUCASS2023-493

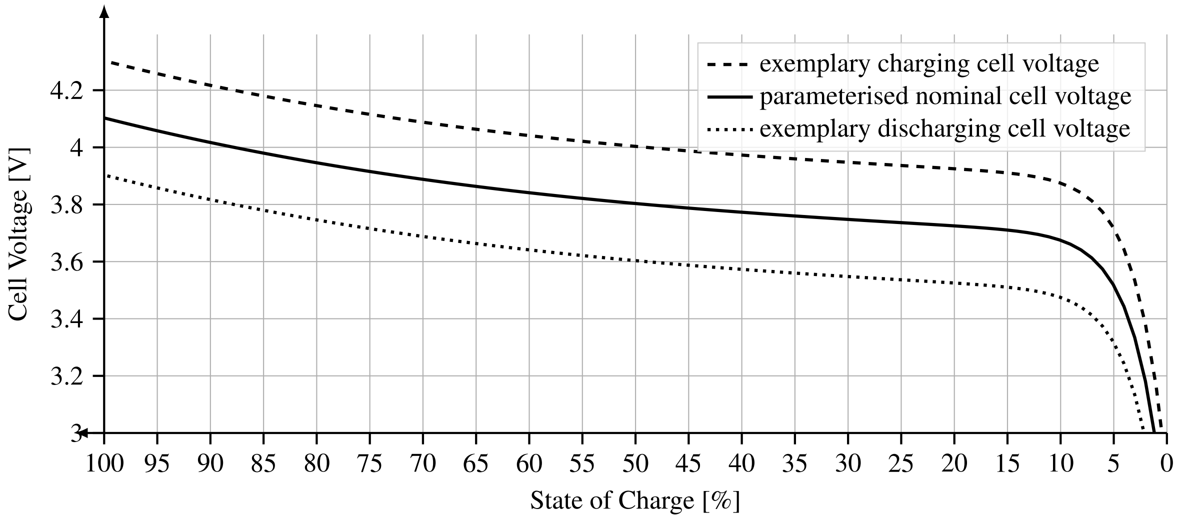

Figure 5: Parameterised battery cell voltages based on data from Chen and Rincon-Mora & Marra *et al.* [27,28]

and accelerate ageing. Secondly, regarding peak power, a maximum C-rate must not be violated. Finally, the individual cell voltage must not fall below the cell cut-off voltage during discharge.
The C-rate ϑ is defined as

$$\vartheta = \frac{I}{C_{nom}}, \tag{4}$$

where I is the discharge current and C_{nom} the batteries nominal energy capacity. The higher the value the faster the battery can be discharged. For this study a value of $\vartheta = 5$ is used.
The values used for the nominal capacity C_{nom} and voltage V_{nom}, as well as of the cut-off voltage V_{min}, are listed in Table 1.

Table 1: Battery main characteristic parameters according to Chen and Rincon-Mora [27]

Parameter	**Symbol**	**Value (Unit)**
Nominal cell voltage	V_{nom}	3.75 V
Cell cut-off voltage	V_{min}	2.5 V
Nominal cell capacity	C_{nom}	2 Ah

To ensure that all three limits are met, the battery total energy capacity may exceed the amount of energy needed, as otherwise e.g. high power demands during the mission would lead to a cell voltage drop below the cut-off voltage or exceed the set C-rate limit. After sizing for the required number of battery cells N_{cells}, the battery mass m_{bat} is calculated by dividing the total battery energy with the assumed pack level gravimetric energy density ρ_{bat} with

$$m_{bat} = \frac{C_{nom} \cdot V_{nom} \cdot N_{cells}}{\rho_{bat}}. \tag{5}$$

2.1.4 Thermal management system modelling

The TMS is an active liquid coolant system, its architecture is depicted in Figure 6. Coolant flows through the components picking up the heat losses of the electric components. A pump is modelled to keep the coolant flowing, which takes some parasitic electric power based on the required coolant flow. To transfer the heat to ambient air the coolant then flows through a heat exchanger. The model accounts for a fan placed in front of the heat exchanger to ensure sufficient airflow. Electric power for the fan is calculated assuming an isentropic compression with fixed efficiency plus an electromechanic efficiency and the pressure loss over the heat exchanger. The masses of the individual parts of the TMS are estimated using mainly empirical relations. Overall, the specific heat rejection rate, which relates dissipated waste heat to the TMS mass, is about 1.5 kW/kg.

DOI: 10.13009/EUCASS2023-493

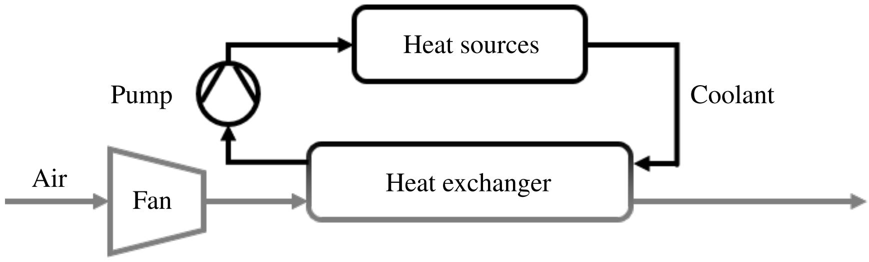

Figure 6: TMS architecture overview adapted from Link *et al.* [30]

2.2 Validation of mission simulation and aircraft model

To ensure that the mission simulation as well as the aircraft model are a valid basis for this retrofit study, the previously described sizing routine is used to size conventionally powered aircraft based on four different missions from the payload range diagram of the ATR 42-500 [31]. Range and payload for the four missions are listed in Table 2. All missions are in the maximum take-off mass zone of the payload range diagram, where a higher range is traded for a lower payload. Two of the missions represent the ends of that range, maximum payload (Mission 1) and maximum fuel mass (Mission 4). All missions include an additional 541 km of range added to the displayed values to account for 87 nautical miles of diversion range plus an additional 45 minutes of flight at cruise conditions as reserve [31].

Table 2: Validation missions and results

		Mission 1	**Mission 2**	**Mission 3**	**Mission 4**
Range	[km]	833	1555	1852	3009
Payload	[kg]	5450	4560	4200	2900
MTOM	[kg]	18603	18608	18604	18728
Fuel mass	[kg]	1909	2794	3155	4573

Range always +541 km to account for reserves

The data used in the aircraft model in all calculations is listed in Table 3. The data includes information on aerodynamics and the propulsion system as well as parameters describing the missions in more detail. These values are also used for the calculations with the battery-electric powertrains when applicable.

The resulting MTOM of the aircraft sized to the four missions - listed in Table 2 - are in very good agreement with the MTOM of the original aircraft of 18 600 kg. All values are within 1 % of the original MTOM, as displayed in Figure 7. The figure also shows the differences in required fuel masses, which are all within 2 % of the original values. These results show that the aircraft model as well as the mission simulation, respectively, are a valid basis for the electric powertrain sizing, for retrofits of this aircraft, to be performed in this study.

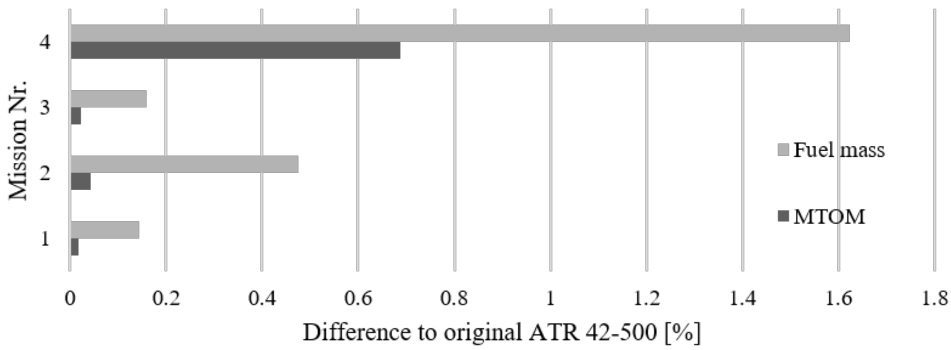

Figure 7: Validation results

DOI: 10.13009/EUCASS2023-493

Table 3: Aircraft model data based on ATR 42-500

	Symbol	Unit	Value
Aerodynamics			
Wing loading	W/S	N/m^2	3348
Zero-lift drag coefficient	c_{D_0}	-	0.023
Zero angle of attack lift coefficient	c_{L_0}	-	0.15
Propulsion			
Turboprop efficiency	BSFC	g/kW/h	270
Propeller efficiency	η_{Prop}	-	0.8
Engine power-to-weight ratio	P/W	W/kg	3500
Aircraft power-to-weight ratio	P/W	W/kg	173
Mass			
Empty mass without engines	EMWE	kg	10330
Maximum take-off mass	MTOM	kg	18600
Mission			
Take-off distance	d_{TO}	m	1290
Climb power setting	ps_{Climb}	-	0.75
Cruise altitude	h_{Cruise}	m	5150
Cruise speed	v_{Cruise}	m/s	142

3. Results and discussion

In this section the results of sizing the aircraft with the battery-electric powertrains are presented. All aircraft are sized for the maximum payload of the original aircraft with 5450 kg. The first study assumes state of the art (SOA) technology. Thereafter, this study assumes technology projections for 2035 and 2050. For both years two scenarios are analysed: a conservative and a nominal one. The data for the scenarios is based on different technology improvement trends, conservative being lower than the nominal scenario. While for the battery the gravimetric energy density is adapted, for motor and power electronics only the power-to-weight ratio is changed. Contrary to the previously in chapter 2 described sizing routines where the mass came from the model, now these values are used to determine component masses. All efficiencies or other model characteristics remain unchanged. Thus, only values that impact the individual component masses are altered. The data used for the different technology projections is listed in Table 4.

Table 4: Technology assumptions

	Unit	SOA	2035		2050		Source
			conservative	nominal	conservative	nominal	
Motor P/W	kW/kg	4.83	10	16.8	11.3	24.3	Pastra *et al.* [32]
Inverter & converter P/W	kW/kg	8.3	10.5	17.45	12	25.2	Hall *et al.* [33]
Battery ED	Wh/kg	250	286	450	393	611	Tiede *et al.* [10]

Firstly, this study showed that retrofitting the battery-electric aircraft to the exact same mission as the conventionally powered aircraft is not possible with any of the aforementioned technology assumptions. A significant reduction in range was necessary. To decrease range and maintain a comparable mission profile, as shown in Figure 2, the cruise altitude had to be reduced as well. Otherwise, only reducing the range portion during cruise would yield a mission where the aircraft climbs to cruise altitude and immediately starts to descend again as no cruise is left. A first mission with significantly reduced range of only about 100 km and a reduced cruise altitude of 2000 m was set up and will be referred to as Mission CO (Comparable to Original) in this paper.

As for the scenarios with lower technology levels still no retrofits were possible – even for Mission CO. The mission requirements were therefore relaxed further and the feasibility of retrofitted battery-electric aircraft for this new mission, namely Mission RE, was analysed. In addition to a further reduction in cruise range and in cruise altitude, the take-off distance was increased and climb power setting as well as cruise speed decreased. All modified parameters for both adapted missions are listed in Table 5. A battery-electric retrofit is possible if the MTOM of the aircraft sized

DOI: 10.13009/EUCASS2023-493

for these adapted missions is equal to the 18.6 t of the original aircraft. If the resulting battery-electric aircraft had an even lower MTOM, the range was increased again until the MTOM matched the originals value again. The results with these adapted mission are presented in the following sections based on the various technology assumptions.

Table 5: Changed mission requirements for battery-electric retrofits

	Unit	Mission CO*	Mission RE*
Take-off distance	m	1290	1500
Climb power setting	-	0.7	0.5
Cruise altitude	m	2000	1000
Cruise speed	m/s	142	100
Minimum cruise range	km	45	45
Total range	km	103	76

*No reserves accounted for in both missions

3.1 State of the art technology assumptions

Using Mission CO results in a battery-electric aircraft with 22 755 kg of MTOM, hence no retrofit possible in this case. This is not to say that designing an aircraft for such requirements is not possible, but rather that it would be heavier than the original aircraft. The mass breakdown for Mission CO is presented in Figure 8. On the aircraft level Figure 8a shows that the powertrain and battery are both more than twice as heavy as the conventional engines and fuel respectively. The powertrain mass breakdown is shown in Figure 8b. One motor on its own with 412 kg is already close to the conventional turboprop engine mass of 460 kg. Together with the other components, the powertrain mass increases by 115 % in total compared to the conventional engines. This leaves only 845 kg for the batteries to reach the MTOM of 18 600 kg. However, the resulting battery mass is 5000 kg with SOA technology.

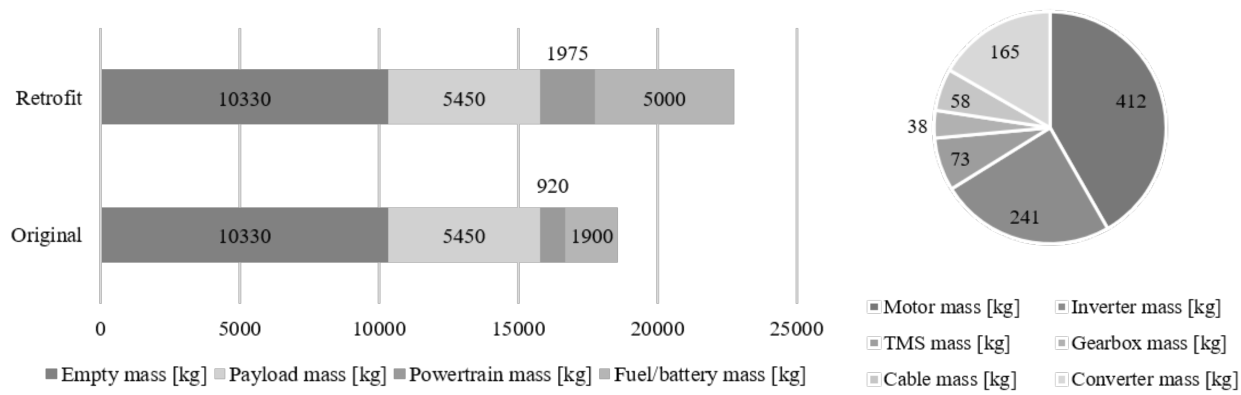

(a) MTOM breakdown

(b) Powertrain unit mass breakdown

Figure 8: Mass breakdown for SOA battery aircraft for Mission CO

The decisive factor for the battery mass is not the energy content but the combination of SOC and power drawn over the mission. Figure 9a shows the power drawn from the batteries over the mission, while Figure 9b and 9c depict the battery SOC and cell voltage profile. As can be seen, the voltage drops to just above the cut-off value of 2.5 V at the end of the cruise phase at around 600 seconds. Carrying less battery mass would result in less capacity. With that, the SOC would be lower earlier on and with the power drawn the cell voltage would fall below the cut-off voltage. Therefore, the battery has to be significantly oversized to avoid violating this limit. At the end of the mission the batteries are still at a SOC of 39.3 %. The aircraft is heavily penalized for carrying this excess energy in form of battery mass, which makes the whole retrofit for this mission unfeasible.
The aircraft resulting from sizing for the Mission RE has a MTOM of 20 426 kg, still 9.8 % too heavy and with that no retrofit is possible. The decisive factor for the battery mass now becomes the required power during take-off, shown in Figure 10a. Only during this power demanding flight phase does the cell voltage nearly reach the cut-off value

DOI: 10.13009/EUCASS2023-493

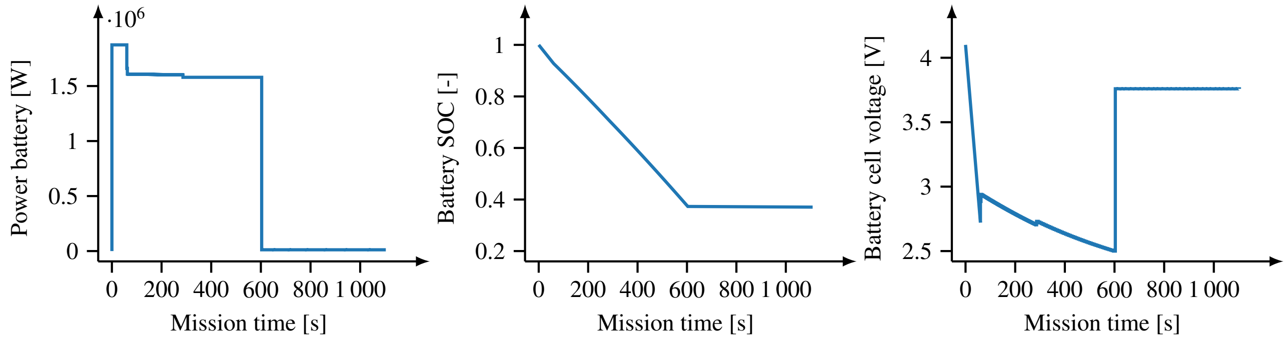

(a) Battery power (b) Battery SOC (c) Battery cell voltage

Figure 9: Mission data SOA battery aircraft for Mission CO

of 2.5 V (cf. Figure 10c). Due to the significantly lowered power demand during cruise in comparison to take-off and climb, the battery can be fully discharged to its minimum SOC of 20 % as per Figure 10b. With the in Table 5 stated range of 45 km for Mission RE the battery was not fully discharged during the mission. As the take-off is the decisive sizing point for the battery the cruise range could be increased to 80 km for a total range of 111 km, where the battery was then fully discharged at the end of the mission. The aircraft sized for Mission RE is lighter and able to fly further than the aircraft resulting for the CO mission. In fact, these results are purely theoretical and serve as indicators to understand the effects of certain mission parameters and TLARs on the design and ideal performance of battery-electric powertrains.

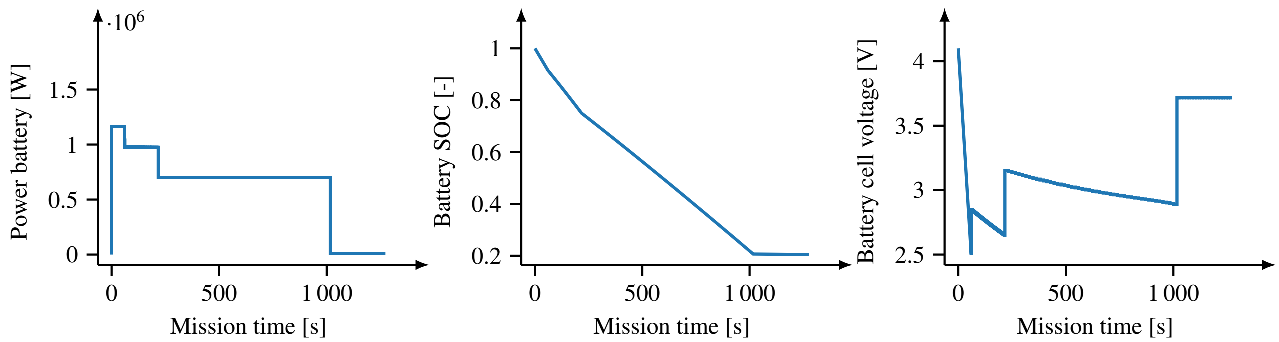

(a) Battery power (b) Battery SOC (c) Battery cell voltage

Figure 10: Mission data SOA battery aircraft for Mission RE

3.2 Conservative technology assumptions for 2035

A battery-electric aircraft sized to Mission CO yields a MTOM of 21 186 kg. The MTOM is 1569 kg lighter than with SOA technology, but still 14 % heavier than the conventional aircraft. The powertrain mass decreases to 1353 kg, which is 47 % heavier than the conventional propulsion system, theoretically leaving 1467 kg for the batteries. The batteries required for the mission, however, would have a mass of 4073 kg. Just as for the SOA technology, at the end of the cruise phase the combination of power drawn and SOC is crucial for the battery sizing due to the cell cut-off voltage limitation. The SOC at the end of this mission is 39 % as well, as the power profile shows the exact same proportions as for SOA technology, only slight lower values as the aircraft is lighter. In conclusion, no retrofit is possible for this scenario either.

Sizing an aircraft to Mission RE with these technology assumptions, the aircraft would have a MTOM of 19 237 kg as a result – 1949 kg lighter than for the CO mission and only 787 kg heavier than the original aircraft. The power, SOC and cell voltage over the mission behave nearly identical to what is shown for the SOA study in Figure 10, only at different absolute values. The take-off is paramount for battery mass again. Due to its high power requirement the cut-off voltage is nearly reached. The battery can be fully discharged to the lower limit of 20 % during cruise again. In this scenario also a cruise range of 80 km and a total range of 111 km are the result for a fully discharged battery.

DOI: 10.13009/EUCASS2023-493

3.3 Nominal technology assumptions for 2035

For Mission CO no retrofit was possible in this scenario either. The aircraft with 18 919 kg of MTOM is still 319 kg heavier than its conventional counterpart. The mass breakdown is shown in Figure 11a. The powertrain of the battery powered aircraft is lighter than the conventional engines. However, the battery is still significantly heavier than the fuel mass of the conventional aircraft – even for this short mission – yielding an overall heavier aircraft. The powertrain mass breakdown in Figure 11b shows lower shares of motors, inverters and converters in comparison to the SOA results in Figure 8b. This is to be expected, as their power-to-weight ratios were increased while TMS, gearbox and cable mass models are not adapted. The behaviour of power, SOC and cell voltage over the mission is similar to the profiles shown in Figure 9. The key limitation for the battery mass is the cell voltage at the end of the cruise phase here as well due to the aforementioned similarity in the mission profile. The battery SOC at the end of the mission is 39 % as before.

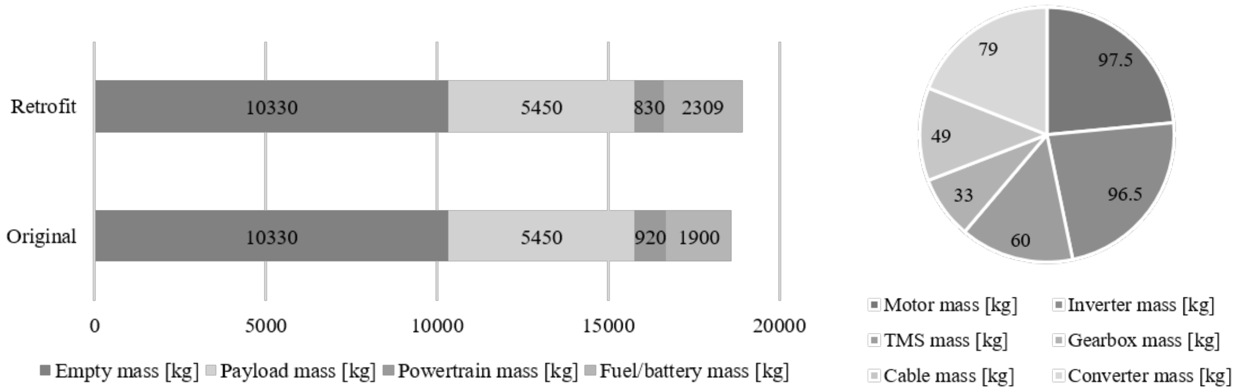

(a) MTOM breakdown

(b) Powertrain unit mass breakdown

Figure 11: Mass breakdown for 2035 nominal battery aircraft for Mission CO

A viable retrofit is possible for the requirements from Mission RE for this technology scenario. The range can be increased slightly from the value listed in Table 5. The aircraft then results in a MTOM of 18 594 kg. A total range of 176 km with 145 km during cruise can be achieved. The power profile over the mission is shown in Figure 12a, the SOC is given in Figure 12b and the battery cell voltage in Figure 12c. In this case the cell voltage is not the limiting factor during the mission, as the cell voltage never drops below 3.2 V, which can be seen in Figure 12b. The battery is solely sized for energy capacity.

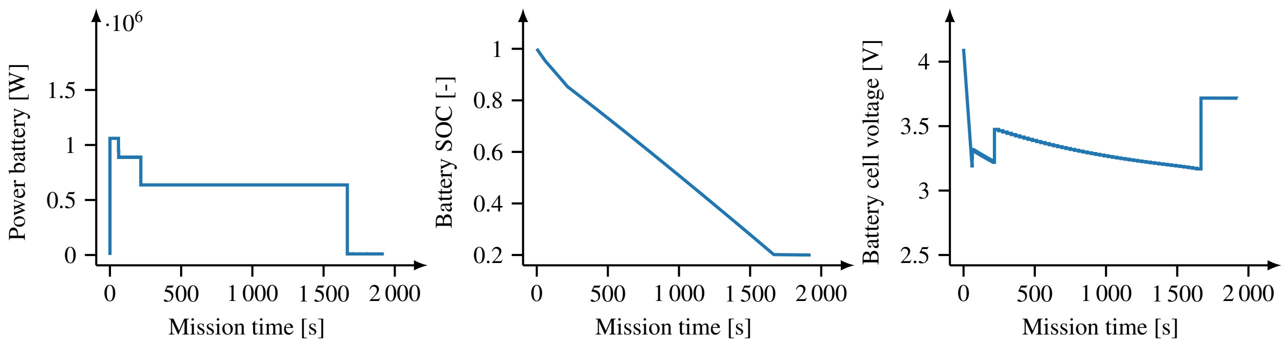

(a) Battery power

(b) Battery SOC

(c) Battery cell voltage

Figure 12: Mission data 2035 nominal battery aircraft for Mission RE

3.4 Conservative technology assumptions for 2050

Once again, a viable retrofit is not possible for this scenario and Mission CO. The aircraft MTOM is 19 652 kg. As for every battery aircraft sized to these mission requirements so far, the cell voltage at the end of cruise is decisive for the battery mass and again the battery can not be fully discharged to 20 % during the mission. A SOC of 39 % remains at the end of the mission.

DOI: 10.13009/EUCASS2023-493

Mission RE allows for a viable retrofit. The technology projections for the 2050 conservative scenario are lower than for the 2035 nominal scenario though (cf. Table 4). Hence, an aircraft with a lower total range of 123 km without reserves is possible here. The trends of power, SOC and battery cell voltage over the mission are similar to the other successful retrofit shown in Figure 12. Only the voltage level is generally slightly lower. There are two reasons for this effect. On the one hand the power-to-weight-ratios for motors and power electronics are lower and therefore the powertrain is heavier. As a consequence, less battery mass can be added to the aircraft. The lower battery mass on its own means lower battery capacity and as a cell always has the same capacity – independent of its mass – the cell number is reduced. These cells share the same load though and therefore the load on each cell is higher and its voltage lower. On the other hand the lower battery energy density intensifies this mechanism, yielding even less capacity and hence cells.

3.5 Nominal technology assumptions for 2050

With these technology assumptions a retrofit is possible for Mission CO and Mission RE that is lighter than the original 18.6 t wherefore the range was increased again to match the MTOM. For Mission CO the result is an aircraft with a powertrain mass of 650 kg and 2170 kg of battery mass, which is able to fly 184 km without any reserves. The power, SOC and battery cell voltage profiles over the mission are shown in Figures 13a, 13b and 13c respectively. Despite the significantly higher power demand on the battery during the whole mission in comparison to Mission RE, the battery cell voltage does not decrease to its cut-off level during the mission. Hence, the battery can be fully discharged to the 20 % minimum. Again an effect of the increased battery capacity, allowing for higher loads to be drawn.

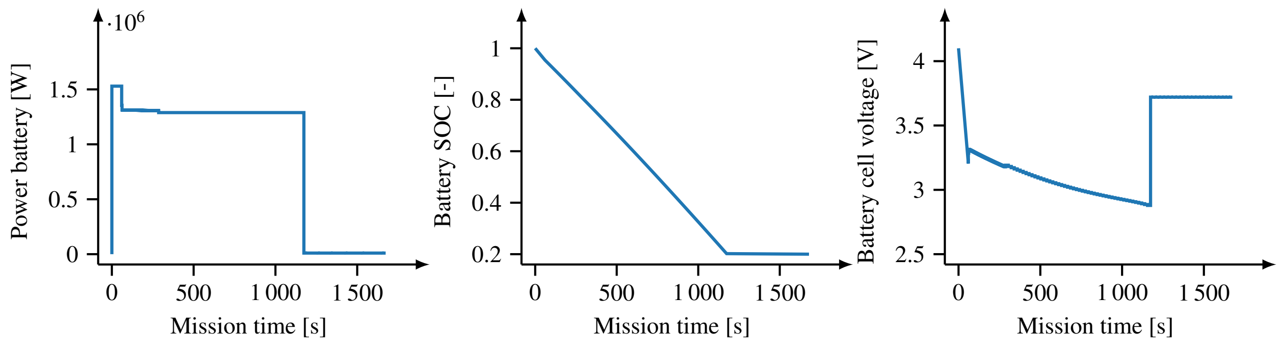

(a) Battery power (b) Battery SOC (c) Battery cell voltage

Figure 13: Mission data 2050 nominal battery aircraft for Mission CO

Mission RE for this technology scenario allows for a battery-electric aircraft that is able to cover 278 km of range without reserves. The MTOM breakdown is depicted in Figure 14a. The powertrain for the battery aircraft is now approximately 30 % lighter than for the original aircraft. The mass breakdown of the powertrain is shown in Figure 14b. Motor and power electronics are only about half the powertrain mass.

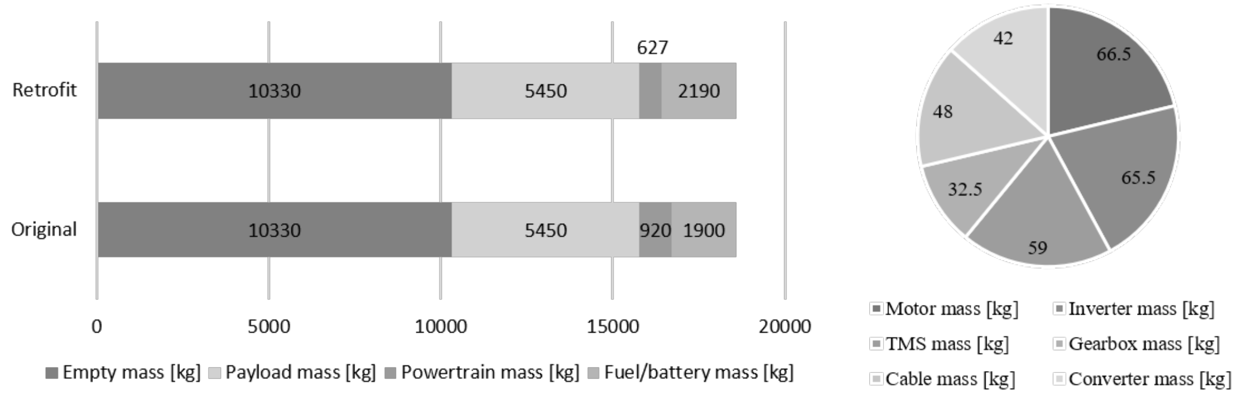

(a) MTOM breakdown (b) Powertrain unit mass breakdown

Figure 14: Mass results 2050 nominal aircraft for Mission RE

DOI: 10.13009/EUCASS2023-493

3.6 Retrofit to original mission requirements

In a final analysis the battery energy density is calculated, which would allow a battery powered retrofit with the exact same mission as the original ATR 42-500 with full payload. The cruise altitude is kept at 5150 m, while the range is set to 833 km plus the additional 541 km to account for reserves.
For all models, except for the batteries, the 2050 nominal assumptions are used. Figure 15 shows the MTOM results of the battery-electric aircraft sized to this mission with increasing battery energy density. The MTOM of the conventional aircraft is being represented by the dashed black line. The black dotted line is at the battery energy density starting value of 611 Wh/kg for the 2050 nominal scenario.
Starting at 52 456 kg for the 2050 nominal scenario, the hypothetical electric aircraft is nearly three times as heavy as the conventional aircraft. The MTOM curve shows a rapid initial decline and reaches 25 033 kg for 1200 Wh/kg, which then evens out with further improvement of the battery energy density. This effect is due to the decreasing share of the battery mass in overall MTOM. At a 20 % share of the battery mass, for instance, a decrease of that mass by 50 % yields an improvement of 10 % in MTOM. At only 10 % share the same improvement of 50 % only results in 5 % total reduction. With 2000 Wh/kg an aircraft with a MTOM of 20 646 kg is the result. To reach the original MTOM of 18 600 kg a 5.6 times higher battery energy density of 3450 Wh/kg is necessary in comparison to the projected value for the 2050 nominal scenario.

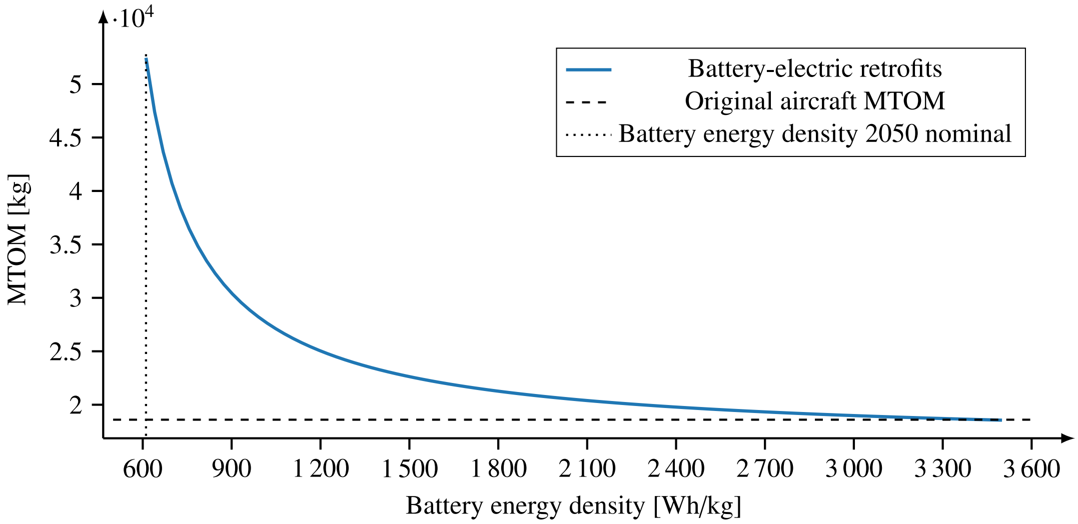

Figure 15: MTOM for retrofit aircraft to original mission as a function of battery energy density

3.7 Summary and discussion

The results of all retrofits for the different technology scenarios in this study are summarised in Table 6. For the lower technology scenarios no retrofits are possible, even with the heavily relaxed mission. Only for the higher scenarios retrofits are possible, but still with significantly reduced ranges in comparison to the original aircraft. The low energy density of the batteries strongly limits the achievable range. For the highest technology assumption, batteries have a higher share in the total MTOM than the fuel for the conventional aircraft, due to the powertrain being lighter than the conventional turboprop engines. Still, in comparison to the conventionally powered aircraft, the range is only about 30 % of the original range while still excluding any reserves. In fact, none of the battery-electric retrofit aircraft would even be able to fly the reserve mission of the original aircraft with 541 km of cruise range.
The powertrain unit mass breakdowns showed decreasing shares of motor and power electronics. For the last scenarios the share of the other components was nearly half the mass. In further studies, future technology assumptions should be used for these other powertrain components as well.
Further, it has to be noted that although the parameterised battery cell voltage curve assumes the characteristic of a lithium-ion cell, the energy densities used in the exploratory technology study exceed values for the most prominent lithium-ion batteries [34]. An updated battery model should be used for such future technology assumptions.

DOI: 10.13009/EUCASS2023-493

Table 6: Summary of the battery-electric retrofit results

Scenario	Mission	Retrofit possible	Range
SOA	Mission CO	No	-
SOA	Mission RE	No	-
2035 conservative	Mission CO	No	-
2035 conservative	Mission RE	No	-
2035 nominal	Mission CO	No	-
2035 nominal	Mission RE	Yes	176 km
2050 conservative	Mission CO	No	-
2050 conservative	Mission RE	Yes	123 km
2050 nominal	Mission CO	Yes	184 km
2050 nominal	Mission RE	Yes	278 km

4. Conclusion

The present paper analysed battery-electric retrofits for medium-sized regional aircraft based on the ATR 42-500. The methodology used and the major component models of the electric powertrain were described. The methodology and aircraft model were successfully validated by sizing conventionally powered aircraft and comparing the results to the original ATR 42-500 aircraft.

Battery electric powertrains are sized as retrofits into the original airframe for three technology levels: State of the art and projections for the years 2035 and 2050. For the future technology projections two development scenarios were considered, a conservative and a nominal one. For each scenario two missions were analysed. Mission CO with only a reduced cruise altitude and range and Mission RE where further requirements such as take-off distance, climb power setting and cruise speed were relaxed.

The study revealed that without major improvements of the electric motor, corresponding power electronics and battery weight, no retrofits are possible as the resulting aircraft were always heavier than the original MTOM.

Retrofits are only possible for significant technology improvements. Firstly, for Mission RE with the significantly relaxed requirements, starting in the 2035 nominal scenario a retrofit was possible. Same for the 2050 nominal scenario for Mission CO. However, with a maximum range of 278 km for the battery-electric retrofit aircraft, the range is significantly reduced to less than 30 % of the conventionally powered aircraft, without accounting for any reserves.

The obtained results show, that battery-electric retrofits in this aircraft category are most likely not viable in the mid-term future without any major technology breakthroughs. The aircraft from the highest technology scenarios might have some potential applications for very short routes like fjord hopping in Scandinavia. In general, clean sheet aircraft designs in this category, utilizing additional benefits of electrified propulsion, e.g. distributed propulsion, will likely offer a more promising approach toward battery-electric regional aircraft with ranges similar to conventionally powered aircraft.

For studies where a retrofit was not possible, the combination of state of charge and power drawn from the batteries resulted in battery limitations due to the cell voltages falling below the cut-off value. For most studies, the batteries therefore had to be oversized regarding energy capacity and could not be fully discharged during the missions. These results highlight the importance of using a comprehensive battery model for sizing electric aircraft to account for these discharge characteristic limitations.

Based on the assumptions made in the paper, a battery energy density of 3450 Wh/kg was identified to be required in the 2050 nominal scenario for a battery-electric regional aircraft in order to fulfill the exact mission specifications of the original ATR 42-500 regarding take-off length, cruise range, cruise altitude, cruise speed and reserves.

5. Acknowledgments

The authors would like to thank Antje Link for her valuable contributions to the powertrain models, especially the thermal management system models, and Stefanie de Graaf for her review and valuable feedback.

DOI: 10.13009/EUCASS2023-493

References

[1] *Flightpath 2050: Europe's vision for aviation ; maintaining global leadership and serving society's needs ; report of the High-Level Group on Aviation Research*. Policy / European Commission. Publ. Off. of the Europ. Union, Luxembourg, 2011.

[2] Air Transport Action Group. Waypoint 2050: Balancing growth in connectivity with a comprehensive global air transport response to the climate emergency: a vision of net-zero aviation by mid-century.

[3] Andreas W. Schäfer, Steven R. H. Barrett, Khan Doyme, Lynnette M. Dray, Albert R. Gnadt, Rod Self, Aidan O'Sullivan, Athanasios P. Synodinos, and Antonio J. Torija. Technological, economic and environmental prospects of all-electric aircraft. *Nature Energy*, 4(2):160–166, 2019.

[4] Ajay Misra. Energy storage for electrified aircraft: The need for better batteries, fuel cells, and supercapacitors. *IEEE Electrification Magazine*, 6(3):54–61, 2018.

[5] PIPISTREL. Velis electro: Electric pioneer. https://www.pipistrel-aircraft.com/products/velis-electro, 2023. Accessed 12-June-2023.

[6] Eviation. Aircraft alice. https://www.eviation.com/aircraft/, 2023. Accessed 12-June-2023.

[7] Brandon Graver, Kevin Zhang, and Dan Rutherford. Co2 emissions from commercial aviation, 2018.

[8] Stefan Baumeister, Abraham Leung, and Tim Ryley. The emission reduction potentials of first generation electric aircraft (fgea) in finland. *Journal of Transport Geography*, 85:102730, 2020.

[9] Martin Hepperle. Electric flight - potential and limitations. In *Energy Efficient Technologies and Concepts of Operation*, 2012.

[10] Blake Tiede, Cody O'Meara, and Ralph Jansen. Battery key performance projections based on historical trends and chemistries. In *2022 IEEE Transportation Electrification Conference & Expo (ITEC)*, pages 754–759. IEEE, 2022.

[11] Markus Aasen Anker and Jonas Kristiansen Noland. Preliminary sizing of a battery-powered all-electric propulsion system for regional aircraft. In *IECON 2022 – 48th Annual Conference of the IEEE Industrial Electronics Society*, pages 1–6. IEEE, 2022.

[12] Trym Bærheim, Jacob J. Lamb, Jonas Kristiansen Nøland, and Odne S. Burheim. Potential and limitations of battery-powered all-electric regional flights—a norwegian case study. *IEEE Transactions on Transportation Electrification*, 9(1):1809–1825, 2023.

[13] Gokcin Cinar. *A Methodology for Dynamic Sizing of Electric Power Generation and Distribution Architectures*. Phd thesis, Georgia Institute of Technology, Atlanta, Georgia, 12.2018.

[14] Daniel P. Raymer. *Aircraft design: a conceptual approach*. American Institute of Aeronautics and Astronautics, Inc.

[15] Snorri Gudmundsson. *General aviation aircraft design: Applied methods and procedures*. Butterworth-Heinemann, Oxford and Waltham MA, first edition edition, 2014.

[16] Egbert Torenbeek. *Advanced aircraft design: Conceptual design, analysis, and optimization of subsonic civil airplanes / Egbert Torenbeek, Delft University of Technology, The Netherlands*. Aerospace series. Wiley, Chichester, West Sussex, United Kingdom, 2013.

[17] D. Felix Finger. *Methodology for Multidisciplinary Aircraft Design under Consideration of Hybrid-Electric Propulsion Technology*. Phd thesis, RMIT University, Melbourne, Australia, 2020.

[18] Martin Staggat, Jonas Ludowicy, Victor Johannes Bahrs, Antje Link, and Stefan Kazula. Modelling of a battery supported fuel cell electric power train topology for a regional aircraft. In *12th EASN International Conference*, Oktober 2022.

[19] Gerald V. Brown, Albert Kascak, Ben T. Ebihara, Dexter Johnson, Benjamin B. Choi, Mark W. Siebert, and Carl J. Buccieri. Nasa glenn research center program in high power density motors for aeropropulsion. 2005.

DOI: 10.13009/EUCASS2023-493

[20] C. N. Reynolds. Advanced propfan engine technology (apet) single- and counterrotation gearbox/pitch change mechanism, final report. 1985.

[21] H Neudorfer. *Weiterentwicklung von elektrischen Antriebssystemen für Elektro-und Hybridfahrzeuge*. PhD thesis, Habilitationsschrift, TU Darmstadt, 2008.

[22] Victor Bahrs, Martin Staggat, and Lars Enghardt. Analytical model for electric machine sizing in electrified aviation. *Deutsche Gesellschaft für Luft- und Raumfahrt - Lilienthal-Oberth e.V.*, 2022.

[23] Juha Pyrhonen, Tapani Jokinen, and Valeria Hrabovcová. *Design of rotating electrical machines*. Wiley, Chichester West Sussex United Kingdom and Hoboken NJ, 2008.

[24] D. Krug. Vergleichende untersuchungen von mehrpunkt-schaltungstopologien mit zentralem gleichspannungszwischenkreis fÃ¼r mittelspannungsanwendungen. 2016.

[25] Seyed Saeed Fazel, Steffen Bernet, Dietmar Krug, and Kamran Jalili. Design and comparison of 4-kv neutral-point-clamped, flying-capacitor, and series-connected h-bridge multilevel converters. *IEEE Transactions on Industry Applications*, 43(4):1032–1040, 2007.

[26] R. A. Barrera-Cárdenas and M. Molinas. Modelling of power electronic components for evaluation of efficiency, power density and power-to-mass ratio of offshore wind power converters. In *Offshore Wind Farms*, pages 193–261. Elsevier, 2016.

[27] M. Chen and G. A. Rincon-Mora. Accurate electrical battery model capable of predicting runtime and i–v performance. *IEEE Transactions on Energy Conversion*, 21(2):504–511, 2006.

[28] F. Marra, Guang Ya Yang, E. Larsen, C. N. Rasmussen, and Shi You. Demand profile study of battery electric vehicle under different charging options. In *2012 IEEE Power and Energy Society General Meeting*, pages 1–7. IEEE, 22.07.2012 - 26.07.2012.

[29] Patrick C. Vratny, Corin Gologan, Clément Pornet, Askin T. Isikveren, and Mirko Hornung. Battery pack modeling methods for universally-electric aircraft. 2013.

[30] Antje Link, Jonas Ludowicy, and Martin Staggat. Assessment of a serial cooling concept for htpem fuel cell systems for aviation applications. In *33rd Congress of the International Council of the Aeronautical Sciences*, November 2022.

[31] ATR. Atr 42-500 brochure. `https://www.aerocontact.com/en/virtual-aviation-exhibition/catalog/76-atr-42-500-a-new-standard-of-excellence`. Accessed 03-April-2023.

[32] Chrysoula L. Pastra, Christopher Hall, Gokcin Cinar, Jon Gladin, and Dimitri N. Mavris. Specific power and efficiency projections of electric machines and circuit protection exploration for aircraft applications. In *2022 IEEE Transportation Electrification Conference & Expo (ITEC)*, pages 766–771. IEEE, 2022.

[33] Christopher Hall, Chrysoula L. Pastra, Andrew Burrell, Jonathan Gladin, and Dimitri N. Mavris. Projecting power converter specific power through 2050 for aerospace applications. In *2022 IEEE Transportation Electrification Conference & Expo (ITEC)*, pages 760–765. IEEE, 2022.

[34] K. M. Abraham. Prospects and limits of energy storage in batteries. *The journal of physical chemistry letters*, 6(5):830–844, 2015.